ASSOCIAZIONE NAZIONALE ITALIANA DI INGEGNERIA SISMICA
ANIDIS
Italian National Association of Earthquake Engineering

XVIII CONVEGNO ANIDIS
L'ingegneria sismica in Italia
ASCOLI PICENO 2019
15-19 Settembre

Seismic Monitoring of Base Isolated Buildings Under Low Intensity Earthquakes

Antonello Salvatori [a], Antonio Di Cicco [a], Paolo Clemente [b]
[a] *University of L'Aquila, DICEAA, Via Giovanni Gronchi 18, 67100 L'Aquila, Italy*
[b] *ENEA Casaccia Research Centre , Via Anguillarese 301, 00123 ROMA*

Keywords: Seismic isolation; in situ monitoring; low intensity earthquake effects; rubber isolators

ABSTRACT
Seismic monitoring of base isolated buildings in order to evaluate dynamic behavior during earthquakes and gain experience on the detailed seismic behavior of isolators in order to experience for future design and analysis is discussed in the paper.
The results of previous seismic monitoring of isolated structures permitted to develop a database, used in the creation of new formulas and reference values for the estimation of the fundamental periods of the structures and the percentage of critical damping during dynamic analyses. The database is very well supplied with data on traditional buildings, but not enough for base isolated buildings. Some structures with seismic base isolation have been monitored during recent strong earthquakes in Italy, namely Amatrice earthquake (2016/08/24, Mw=6.0) and Norcia earthquake (2016/10/30, Mw=6.5) and aftershocks.
For these structures, amplification phenomena have been observed up to about twice the accelerations on the superstructure, for very low energy value inputs. In these cases, however, monitoring revealed amplified accelerations extremely small, and very far from being able to damage the structure. Records from the ENEA permanent accelerometric network, installed on the structure under examination, and the tests carried out on the same isolators used for the qualification tests of elastomeric isolators positioned below the analyzed structure, describe the behavior of the isolators in terms of force and displacement defining two non-linear laws, derived from experimental data.

1 INTRODUCTION

It's well known that seismic isolation of a structure, decoupling ground motion from super-structure motion represents still now the better solution to prevent both collapse condition (expecially if the structure is designed according to capacity design) and any level of damage to building structure, infills and plants (Martelli A., Clemente P., Saitta F. and Forni M., 2012).

Its realization usually is done by a physical detachment in the structure which is then divided into two parts: the substructure, rigidly connected to the ground and which must have noticeable low stiffness properties, and the superstructure, which, according to recent studies, must conceive capacity design for its elements (beams, pillars, walls). Seismic isolation, instead of increasing the capacity of the structure, use RID's strategy, drastically reducing the energy transmitted from the ground to the building (Martelli A., Clemente P., 2015).

The substructure, which normally must be realized with high shear stiffness, in order to reduce undesired relative displacements and deformations, and to minimize the main modal period of vibration relevant to substructure itself, has roughly the same acceleration of the ground and must be designed in elastic field (like a rigid body), while the superstructure benefits from the increased deformability resulting from the introduction of isolating devices, obviously with respect of capacity design concepts in order to avoid nonlinear behaviour in case of an exceptional seismic event (Clemente P. and Buffarini G., 2010).

Typically, response spectra in terms of accelerations of most earthquakes have a strong amplification in the range 0.1÷ 0.8 sec, in correspondence of the main vibration period of many traditional buildings (in particular, concrete cast building), (Çelebi M., Bazzurro P.,

Chiaraluce L., Clemente P., Decanini L., De Sortis A., Ellsworth W., Gorini A., Kalkan E., Marcucci S., Milana G., Mollaioli F., Olivieri M., Paolucci R., Rinaldis D., Rovelli A., Sabetta F. and Stephens C., 2010).

Assuming, for simplicity's sake, that the isolators have a linear elastic or comparable behaviour, (in particular when considering collapse prevention or life safety, i.e. for great displacements) the increase of global deformability due to their linear and nonlinear behaviour increases the own modal period of the structural system (Substructure-isolating system-superstructure), moving it towards the area of spectral lower acceleration.

As a result, the earthquake-generated accelerations on the isolated structure are drastically lower than those relevant to the fixed-base configuration, so it's well known that the structure can be easily designed to withstand extreme earthquakes without damage both in structural and in non-structural components, in particular infills and plants (Martelli A., Clemente P., Benzoni G., 2017).

Of course, an increase in fundamental period means also an increase in displacement, but the large component of displacement is localized in the isolating devices, independently from typology and technology, and most of the energy of the earthquake is low-pass filtered and also, in part, dissipated (by elastic cycles in the case of elastomeric isolators, or by friction in the case of pendulum devices, De Stefano A., Matta E., Clemente P., 2016).

From analysis of experimental data on isolated structures, performed in the present study in many buildings, however, it has been noticed that for low acceleration values (like those in areas sufficiently far from earthquake epicentres) the whole system presents vibration periods not suited to those of an isolated structure, due to different displacements and excitation frequency, according to greater stiffness of elastomeric devices (well known phenomenon in rubber or to static friction in pendulum devices), but almost closer to the ones of a fixed base traditional structure, as can be observed from recordings of low energy seismic events carried out by the authors in the structure under examination (Clemente P., 2002).

In figure 1 Arias intensity versus frequency of the system is shown. The Arias intensity (1) is an integral parameter, obtained as cumulative measure of seismic motion during its duration, and it represents the energy at the base of the structure.

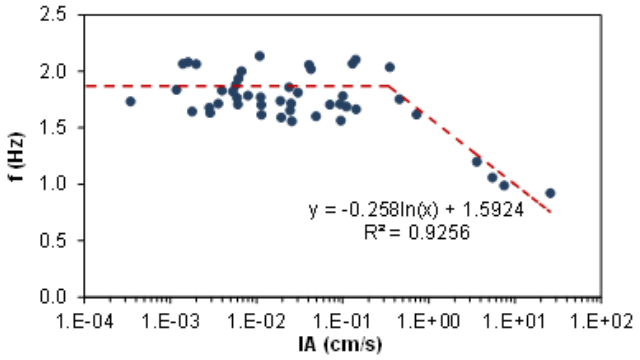

Figure 1. Base energy/frequencies

$$\mathrm{IA} = \frac{\pi}{2g} \cdot \int_0^t a_x^2 + a_y^2 + a_z^2 \; dt \qquad (1)$$

Corresponding to low input energies at the base of the structure, the equivalent stiffness of the structure itself leads to frequency values different from those for which it was designed (< 0.5 Hz). The reduction of the modal vibration period typically increases the seismic acceleration more than the case of higher periods (Bongiovanni G., Buffarini G., Clemente P., Saitta F., De Sortis A., Nicoletti M., Rossi G., 2015).

These accelerations are higher than those evaluated in the design with consequent possible damage to the superstructure (referring to a low damage level, expecially for infills and plants).

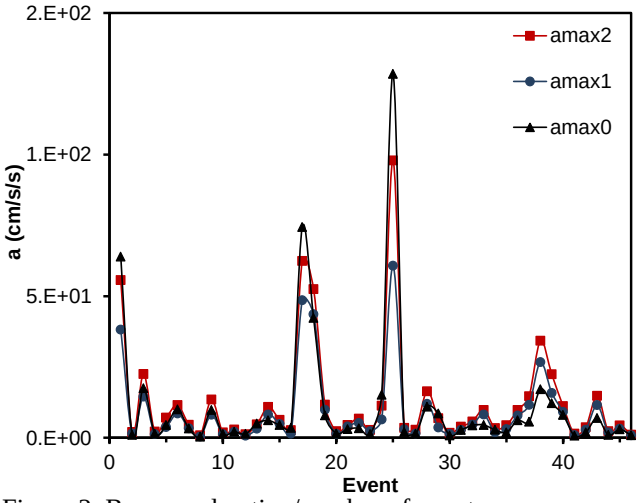

Figure 2. Base acceleration/number of events

In figure 2 the accelerations recorded on the structure at levels 0 (structure solidary to the ground), 1 (at the first level) and 2 (in correspondence of the cover), is shown.

For events characterized by small base acceleration there is an amplification of the acceleration from the bottom upwards, which not represents the expected behaviour for isolated buildings under high intensity excitation.

The two acceleration peaks are related respectively to the earthquake of Amatrice (2016/24/08, M_w 6.0) and Norcia (2016/30/10, M_w 6.5), and they have been recorded near the city of Foligno (Umbria region), about 42 km from Norcia end 60 km from Amatrice.

2 BEHAVIOUR OF FOLIGNO REGIONAL CIVIL PROTECTION CENTER DURING FAR EARTHQUAKES

The regional civil Protection centre of the Umbria region, is located in Foligno (Salvatori A., Di Cicco A, Clemente P., 2019)

The Regional Centre is composed by a building (operative room, analysed in detail in the present work, figure 3), a regional building (emergency and training) where the Special Office for Reconstruction (Umbria Region) is currently located and a third building (Amphitheatre – Plants building).

The first two buildings are seismically isolated (and actually monitored by ENEA) and the third is a traditional one (Bongiovanni G., Buffarini G., Clemente P., Saitta F., Serafini S., Felici P., 2016).

The main structure (Operation room building, figure 3), considered in the present work, has three floors above ground and a basement for a total area of about 1532.25 m^2 above ground, and a volume equal to 8,630.00 m^3;

The structure is in reinforced concrete, with a dome space composed by ten main concrete arches, and is seismically isolated by ten high damping elastomeric isolators, located externally on the ground floor.

The size of the dome is 22 meters in height and 31 meters in diameter base.

The isolated superstructure has a dome supported by ten half arches with cross section 40 x 120 cm, converging towards a single ring from which two concentric cylinders of 16 cm thickness are suspended, with a prestressed reinforced concrete.

The two concentric cylinders have inside a spiral staircase and an elevator placed inside the innermost cylinder. The inner most cylinder and the outermost one are suspended, with a sufficient interface towards the soil so that they can freely move during earthquake.

The outermost cylinder stops at the height of the first floor while the innermost cylinder continues to the basement, at a height of -4.00 m.

The foundation system consists of plinths based on four piles each, linked together by a reinforced concrete beam with cross section 80 x 80 cm, and by radial beams converging in a ring beam with cross section 50 x 140 cm and diameter, measured on the longitudinal axis, equal to 7.20 m inside which descends, until the basement, the elevator core.

Figure 3. Operation room building

There is no connection between the elevator core and the ring beam above.

Above the beams connecting the plinths there is a 20 cm thick slab which is also the base of the dome.

The pedestrian access to the structure is possible by means of a slab (18 cm thickness) that extends as a cantilever from the core elevator suspended on the base of the dome. There is no connection between the slab for pedestrian access and the base of the structure.

Above the foundation plinths, there are 10 concrete supports on which the elastomeric isolation devices are fixed (figure 4, 5).

The floors, with a radial dimension descending from the bottom towards the top of the structure, are supported by circular and radial beams that connect the half arches to the outer vertical cylinder.

Figure 4. Support of an isolator during the construction

Figure 5. Support of an isolator after its completion

In the innermost cylinder are also contained the plants of the various levels down to the basement level which remains separate, and therefore suspended, by the foundation.

The two upper floors are used as offices for the Civil protection operative room and more precisely:

- The first floor consists of 14 offices, in addition to the services and organized through furniture-equipped walls;
- The second floor is divided into a meeting room of about 145.50 m^2, a direction hall of about 60.00 m^2, a meeting hall of about 136.60 m^2 and services.
- The third floor contains other offices and a room for air conditioning systems.

3 BASE ISOLATION SYSTEM AND HIGH DAMPING RUBBER ISOLATOR

The isolators are elastomeric one with soft-type rubber, namely SI-S 1000/240. Their mechanical characteristics are shown in table 1.

Type test were performed for the determination and control of the isolator characteristics (table 1), (Clemente P., Bongiovanni G., Benzoni G., 2017).

Table 1 – Mechanical properties of rubber isolators

External diameter	D_g	1000	mm
Total high without anchorage plates	H	392	mm
Total high with anchorage plate	H	472	mm
Volume of the nucleus	Vol	307.88	dm^3
Total weight without anchorage	W	1834	kg
Maximum horizontal force with maximum seismic displacement	F_{xy}	497	kN
Maximum seismic uniform pression = V / A'	$\sigma_{v\,s,max}$	**3.98**	Mpa
Mimimun sesismic uniform pressure = V_{min} / A'	$\sigma_{v\,s,min}$	**0.00**	Mpa
Vertical stiffness = $E_c \cdot A' / t_e$	K_v	**2310**	kN/mm
Horizontal equivalent stiffness = $G_{din} \cdot A \cdot t_e$	K_e	**1.31**	kN/mm
Stiffness ratio	K_v/K_e	**1764**	

In this case was evidenced an increasing cyclical stress at constant frequency and the corresponding strength of resistance of the isolator.

Being the test carried out on isolators of dimensions equal to half of the installed ones, their mechanical properties are then related to the real dimension of installed isolators.

These test have been fundamental in order to obtain the real nonlinear shear / displacements relation under dynamic testing, which revealed a greater stiffness for low deformations, and consequently a very different hysteretic behaviour which permitted further nonlinear analysis shown in this paper.

For low shear deformation the curve are nonlinear and their stiffness doesn't fit to usual linear stiffness of isolators under life safety or collapse prevention condition.

The results reported the following values for the shear resistance module and damping (figure 6), putting into evidence the variability of lateral stiffness with deformation (figure 7);

the devices have an increase in the damping and in the shear stiffness modulus with the decrease in the lateral deformation.

In particular, for a deformation values from 30% to 5%, there is a sharp increase in stiffness and damping values.

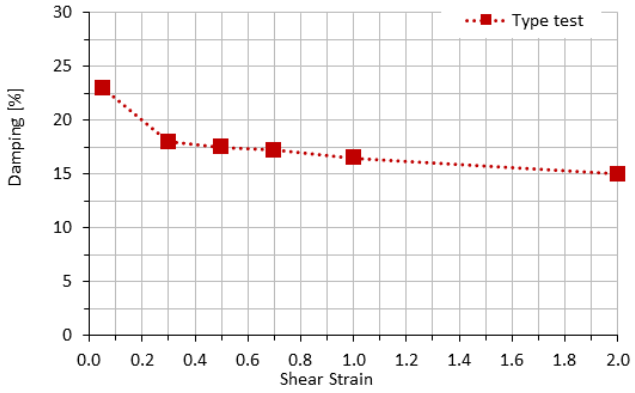

Figure 6. Damping variation as strain varies

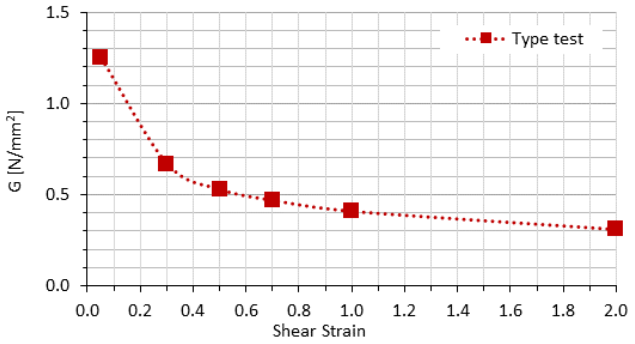

Figure 7. Shear modulus variation as strain varies

4 THE MONITORING SYSTEM

In order to monitor the structure a control equipment was installed in August 2014, with:

- Acquirer Kinemetrics K2, absolute timing using GPS, equipped with 24-bit A/D converter (digital analogue), 12 acquisition channels, 3 of which are connected to the sensor triad in-side the acquirer and 9 connected to the external sensors;

- 12 Sensors Kinemetrics Type Force Balance with dynamic > 120 DB and full scale 2 G, three of which, orthogonal each other, are contained in the acquirer; the remaining 9 are arranged at the level of the first deck, below the floating floor (also used for cable passage).

The instrumentation is arranged on the structure in elevation (figure 8) and in plan (figure 9), where the arrows indicate direction and positive sensors and the point corresponds to the arrowhead, so the sensors for the channels A02, A04, A05 and A06 are vertical.

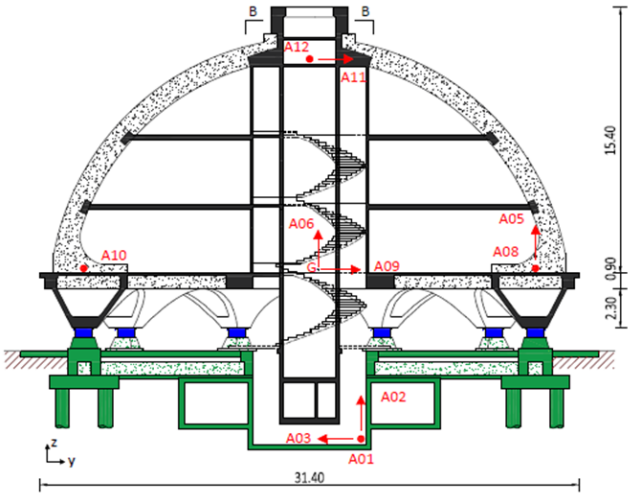

Figure 8. Position in elevation of the instrument and fixes installed

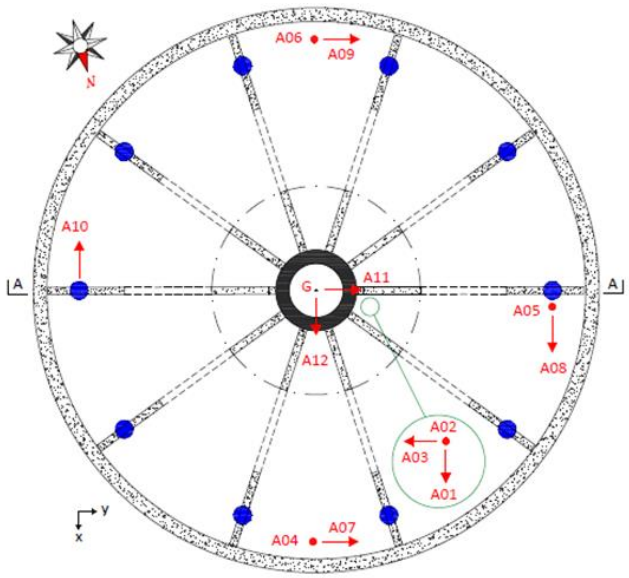

Figure 9. Plant arrangement of installed equipment

The sensor group inside the acquirer, A01, A02 and A03, is positioned below the isolating plane, in the lowest attainable position, near the terminal part of the Elevator Core, so they are measuring soil input under earthquake condition (Clemente P., Bongiovanni G., Buffarini G. and Saitta F., 2016).

The positioning of sensors on the structure, the accelerometers relative to the channels from A04 to A10, is located to the share of the first deck, immediately above the isolating plane, (figure 10), while the sensors related to channels A11 and A12 are positioned at the top of the inner core (figure 11).

They can show properly global behaviour of the building

The recognition of seismic events is carried out in STA/LTA logic (Short Term Average/Long Term average), i.e. by comparing the mean signal measured by each sensor, filtered pass 0.1-10 Hz band, in a short time interval, in this case 0.6 s, (STA) and the mean signal rate detected by the same sensor, band pass filtered 0.1-10 Hz, in a long time interval, in this case 60 s, (LTA). If the STA/LTA value exceeds a preset value, in this case equal to 4, the signal from the channel generates a trigger command.

To reduce the amount of recorded spuria signals, the trigger condition for a single channel is not sufficient to initiate the recording.

To start the recording a determined number of sensors must exceed simultaneously trigger conditions.

In this case were delegated to this task the sensors at the base and the two sensors at the top, clearly less affected by local disturbances.

If 2 Sensors exceeds at the same time the trigger condition starts recording on a card of memory PCMCIA internal to the acquirer.

Figure 10. Accelerometers (A04 – A07) below the floating floor

Figure 11. Accelerometers (A11 – A12) in internal core top.

To record the entire signal the acquirer adds to the head of the recording the portion of the signal prior to the trigger for a preset duration, in this case 30 s.

The detected event is considered terminated when the selected sensors check the condition of detrigger, i.e. the signal amplitudes fall below a preset value, in this case the 40% of the trigger conditions.

Starting from the time of detrigger, the acquirer still continues the recording for a preset time, post event, in this case 30 s.

5 SEISMIC EVENTS RECORDED BY THE ACCELEROMETRIC EQUIPMENT

In table 2 are reported all the seismic event recordings with M_W or $M_L \geq 4.0$ concerning the seismic sequence started on August 24, 2016 (with an event of magnitude M_W= 6.0) until 31 December 2017, which represents all the main earthquake in the latest seismic cluster of central Italy.

The report of the events defined from time source, localization (latitude, longitude, depth), the source of the data (Seismic Bulletin INGV), the name of the registration (ENEA internal code for the archiving of events), the epicentral distance and eventual notes (table 2).

The recorded data requires different calculations in order to extract only data relevant to significant earthquakes recorded in the rea of the isolated building.

The seismic events are selected (table 2), and the relevant data used in order to perform several computational analyses.

Table 2. Recorded events

SOURCE Time [Utc]	Latit.	Longit.	Depth [km]	Magnitude	D_{Epi} [Miles]
24/08/2016 01:36:32	42,698	13,234	8.1	6.0-Mw	53
24/08/2016 01:56:01	42,601	13,276	7.7	4.3-Mw	62
24/08/2016 02:33:29	42,792	13,151	8.0	5.4-Mw	41
24/08/2016 03:40:11	42,614	13,244	10.7	4.1-Mw	59
24/08/2016 04:06:51	42,771	13,124	6.2	4.4-Mw	41
24/08/2016 11:50:31	42.82	13.16	9.8	4.5-Mw	41
24/08/2016 17:46:09	42,659	13,215	10.3	4.2-Mw	54
24/08/2016 23:22:06	42,654	13.21	11.8	4.0-Mw	54
25/08/2016 03:17:17	42,745	13,193	9.0	4.3-Mw	47
25/08/2016 12:36:05	42.6	13,282	7.5	4.4-Mw	63
26/08/2016 04:28:26	42,605	13,292	8.7	4.8-Mw	63
27/08/2016 02:50:59	42,843	13,238	7.8	4.0-Mw	46
28/08/2016 15:55:35	42,823	13,232	8.7	4.2-Mw	46
03/09/2016 01:34:12	42.77	13,132	8.9	4.2-Mw	41
03/09/2016 10:18:51	42,861	13,217	8.3	4.3-Mw	43
16/10/2016 09:32:35	42,748	13,176	9.2	4.0-Mw	47
26/10/2016 17:10:36	42.88	13,128	8.7	5.4-Mw	36
26/10/2016 19:18:06	42,909	13,129	7.5	5.9-Mw	35
26/10/2016 21:42:02	42,863	13,121	9.9	4.5-Mw	36
27/10/2016 03:19:27	42,843	13,143	9.2	4.0-Mw	38
27/10/2016 03:50:24	42,984	13.12	8.7	4.1-Mw	34
27/10/2016 08:21:46	42,873	13,097	9.4	4.3-Mw	34
27/10/2016 17:22:23	42,839	13,099	9.0	4.2-Mw	35
29/10/2016 16:24:33	42,811	13,095	10.9	4.1-Mw	36
30/10/2016 06:40:17	42,832	13,111	9.2	6.5-Mw	36
30/10/2016 07:34:48	42,922	13,129	9.9	4.0--ML	35
30/10/2016 11:58:17	42.84	13,056	10.2	4.0-Mw	32
30/10/2016 12:07:00	42,845	13,078	9.7	4.5-Mw	33
30/10/2016 13:34:54	42,803	13,165	9.2	4.1-Mw	42
30/10/2016 18:21:09	42.79	13,152	9.6	4.0-Mw	42
31/10/2016 03:27:40	42,766	13,085	10.6	4.0-Mw	38
31/10/2016 07:05:45	42,841	13,129	10.0	4.0-Mw	37
01/11/2016 07:56:40	43	13,158	9.9	4.8-Mw	37
03/11/2016 00:35:01	43,029	13,049	8.4	4.7-Mw	29
12/11/2016 14:43:34	42,723	13,209	10.1	4.1-Mw	49
14/11/2016 01:33:44	42.86	13,158	11.0	4.0--ML	39
29/11/2016 16:14:03	42,529	13.28	11.1	4.4-Mw	68
11/12/2016 12:54:53	42.9	13,113	8.3	4.3--ML	34

All the acquired data are extracted according to the following processing, to be carried out for each recording:

- Transformation of data from acquirer units, Volt, into CM/s/s units.
- Calculation and graphical representation of Fourier transforms to select the filtering frequencies.
- Instrumental correction for the characteristics of each sensor, natural frequency and damping, with a change of direction for sensors related to CH03 and CH10, frequency filtering and dual integration to obtain the temporal histories corrected in terms of acceleration, speed and displacement.
- For magnitude $\geq$ 5.0, the calculation of the Accelerometric Group response spectra at the base was also carried out.
- For all recordings, the maximum, in acceleration and displacement, for each channel, was calculated, the maximum for each recording and the channel on which that value was obtained (table 3), showing the maximum acceleration values expressed in cm/s^2.

Table 3 – Maximum acceleration values of recorded events

Rec	CH01	CH02	CH03	CH04	CH05	CH06	CH07	CH08
TN015	59.9	27.2	43.4	42.3	37.7	40.1	40.4	36.1
TN018	0.9	0.5	0.7	0.9	0.7	0.7	1.6	1.0
TN032	16.9	9.0	14.9	16.2	12.8	13.7	10.9	14.1
TN045	1.1	0.7	1.3	1.2	1.2	1.0	1.2	1.3
TN047	3.3	2.1	4.4	4.9	3.9	4.4	3.9	3.0
TN066	7.3	5.2	8.7	6.6	7.4	7.0	7.5	9.8
TN074	2.5	1.8	2.4	2.1	2.0	1.7	3.4	2.5
TN078	0.3	0.2	0.3	0.4	0.4	0.4	0.5	0.2
TN080	6.6	2.7	9.3	5.2	6.7	4.9	7.9	4.8
TN083	0.9	0.5	1.3	0.9	0.8	0.8	1.3	1.1
TN086	2.0	1.1	1.9	2.0	1.4	1.6	2.2	1.5
TN093	1.3	0.5	0.8	0.7	0.7	0.7	0.6	0.8
TN102	4.5	2.1	4.2	3.7	2.8	2.9	3.0	2.6
TO015	5.1	3.4	5.8	3.3	2.9	4.8	9.1	4.8
TO017	4.5	1.5	2.1	2.2	2.3	2.0	2.7	5.3
TP016	2.6	1.3	2.8	2.3	2.0	2.0	1.4	1.2
TP021	67.6	26.2	51.4	27.3	24.6	21.7	44.3	22.7
TP026	36.3	21.5	37.3	35.4	28.2	30.4	44.8	36.1
TP053	7.7	2.7	7.2	4.9	4.4	4.3	8.1	6.0
TP071	1.5	1.0	0.9	1.6	1.3	1.9	1.3	1.1
TP073	1.8	1.7	3.0	2.4	2.2	2.3	3.3	3.9
TP086	3.2	1.7	3.3	3.3	2.4	2.3	5.2	5.0
TP103	1.0	1.0	1.2	1.5	1.2	1.4	2.4	1.8
TP144	12.4	6.8	8.9	8.3	8.2	7.1	4.1	7.6
TP151	74.8	61.6	118.4	67.0	70.7	67.6	60.0	42.4
TP170	1.4	1.3	2.0	2.0	1.1	1.2	3.0	1.5
TP235	1.4	1.2	1.2	2.1	1.8	1.8	1.7	1.0
TP237	6.3	6.4	10.9	8.2	8.6	7.1	11.3	5.5
TP251	7.4	4.4	4.4	4.2	3.4	3.5	3.3	2.9
TP275	0.5	0.4	0.7	0.6	0.5	0.4	1.2	0.8
TP310	2.6	1.5	2.7	2.2	1.8	2.1	2.1	2.8
TP322	3.3	3.4	3.9	4.3	4.0	3.8	4.5	1.8
TP354	4.1	2.9	4.1	5.9	4.7	5.5	6.2	8.5
TQ077	1.7	0.8	2.7	1.3	1.3	1.3	1.7	1.9
TQ092	1.7	1.0	1.4	1.5	1.6	1.5	2.2	2.9
TQ171	6.2	2.0	5.5	3.2	3.6	3.4	4.2	8.0
TR018	3.6	2.2	5.6	2.6	2.6	2.4	11.6	4.7

Rec	CH09	CH10	CH11	CH12	Max	Ch
TN015	33.5	35.9	51.0	46.5	59.9	CH01
TN018	1.4	1.2	2.0	1.3	2.0	CH11
TN032	12.3	14.5	22.2	18.5	22.2	CH11
TN045	1.3	1.2	2.1	1.4	2.1	CH11
TN047	3.7	3.5	7.1	4.0	7.1	CH11
TN066	8.0	7.7	10.5	11.2	11.2	CH12
TN074	3.3	2.1	4.6	2.8	4.6	CH11
TN078	0.5	0.3	0.8	0.3	0.8	CH11
TN080	8.9	5.8	13.3	8.5	13.3	CH11
TN083	1.2	1.0	1.6	1.5	1.6	CH11
TN086	1.7	1.6	2.9	2.0	2.9	CH11
TN093	0.7	0.6	1.1	1.0	1.3	CH01
TN102	3.4	2.4	4.6	3.3	4.6	CH11
TO015	7.7	5.3	10.8	6.0	10.8	CH11
TO017	2.7	4.7	3.7	6.3	6.3	CH12
TP016	1.6	1.5	2.4	1.9	2.8	CH03
TP021	48.2	23.6	62.1	37.9	67.6	CH01
TP026	42.4	32.1	51.1	36.3	51.1	CH11
TP053	9.3	6.1	10.7	7.6	10.7	CH11
TP071	1.7	1.1	2.3	1.3	2.3	CH11
TP073	3.5	3.1	4.3	4.3	4.3	CH11
TP086	4.6	4.8	5.9	5.8	5.9	CH11
TP103	2.1	1.4	2.7	2.0	2.7	CH11
TP144	3.4	7.0	7.3	9.3	12.4	CH01
TP151	60.4	46.6	96.0	61.6	118.4	CH03
TP170	3.0	1.5	3.5	1.9	3.5	CH11
TP235	1.3	0.8	2.8	1.4	2.8	CH11
TP237	11.6	5.6	16.4	7.6	16.4	CH11
TP251	3.6	3.1	5.6	5.8	7.4	CH01
TP275	1.3	0.7	1.7	0.8	1.7	CH11
TP310	2.2	2.7	3.3	3.6	3.6	CH12
TP322	4.8	1.9	5.7	3.0	5.7	CH11
TP354	6.2	8.1	8.6	9.4	9.4	CH12
TQ077	1.9	2.1	3.1	2.4	3.1	CH11
TQ092	2.6	2.9	3.7	3.5	3.7	CH11
TQ171	3.2	7.6	6.1	9.8	9.8	CH12
TR018	11.6	4.5	14.2	5.4	14.2	CH11

The event which gave the major values had magnitude M_W = 6.5, registered under the name TP151 (Norcia earthquake PG of 30/10/2016).

This event is discussed in more detail, and can be considered representative of the whole dynamics at the structure under low intensity excitations.

To test the finite element model implemented and the isolator characteristics, the event recordings were also used with the name TN015, relative to the effects of the event of 24/08/2016 with magnitude M_W= 6.0 with epicentral zone near Amatrice (RI).

5.1 Recording analysis TP151

The comparison between the temporal histories of the accelerations at the three monitored levels and for the two directions, (figure 12), shows that seismic actions are different in both directions.

Moving from the ground motion to the motion above the isolator plane, there is a decrease in the amplitude of the accelerations and a noticeable lowering of the frequency content.

Moving from the level above the isolator plane there is an increase in accelerations, which are still lower than those of the ground.

The dominant frequency appears to be still the same but it is evident, more in the direction of CH11, the presence of higher frequencies.

Also the analogous comparison between the Fourier spectra shows that the frequency content in the two measuring points above the isolator plane, CH08 and CH12 in one Direction and CH07 and CH11 in the other direction, is substantially identical, for each direction, below 2 Hz, with the exception of two components in which a higher frequency is detected by the instruments, at about 10 Hz.

In the direction of Ch07 and Ch11 a significant frequency content is evidenced between 7 and 9 Hz, even dominant for Ch11. Such frequency content is not justified in a structure with seismic isolation at the base (figure 13).

A cross spectral analysis is then performed for various channel data.

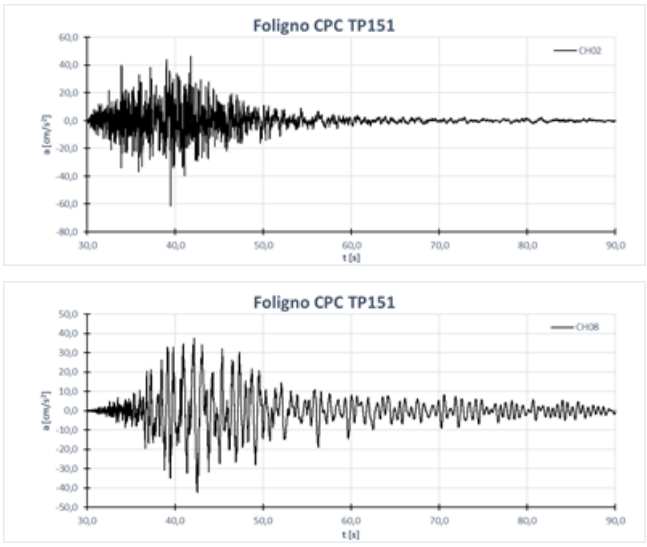

Figure 12. TP151 comparison of the time history signals

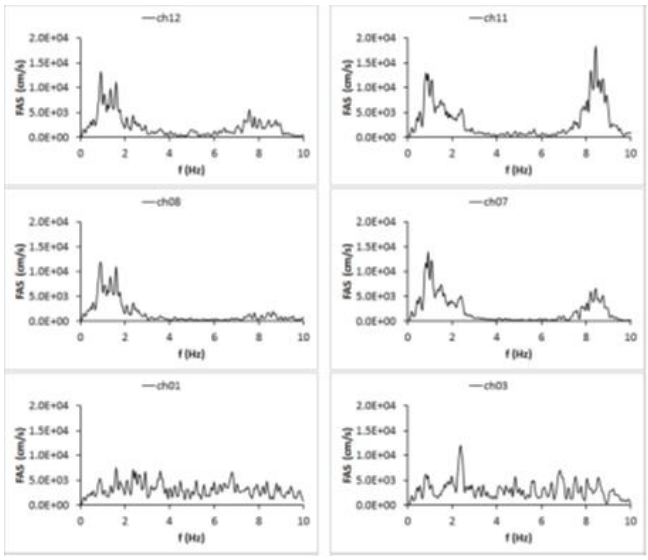

Figure 13. TP151 comparison of the Fourier spectra of accelerations

Cross-spectral analysis, Ch08 Ch12 and Ch07 Ch11, stresses that the motion of the structure above the isolator plane increases very little by proceeding upwards in the range in frequency less than 2 Hz, and it is also consistent and in phase.

This frequency range can be considered representative of the motion of the isolated structure.

The frequency content between 7 and 9 Hz has much greater amplitudes on the top of the structure and in the direction of Ch11, which decrease by going downwards; consistency is high and the motion of the two points of measurement is in opposition to phase. It can be stressed that the motion at these frequencies is originated within the isolated superstructure (figure 14).

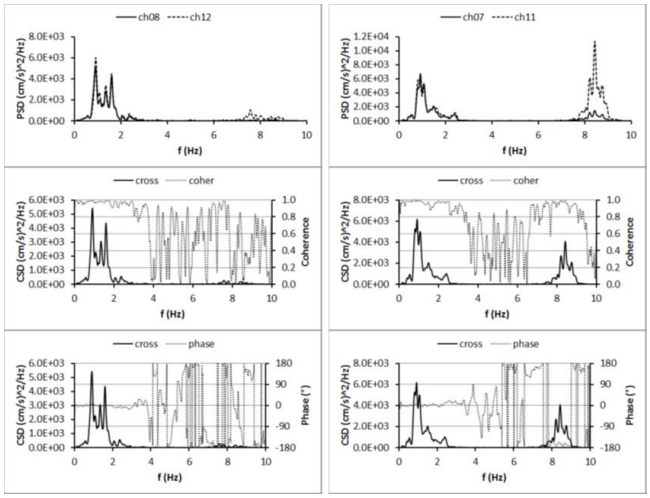

Figure 14. TP151 Cross spectral analysis

To explain the presence of several frequency peaks in the recordings examined, a time-frequency analysis was carried out for the CH11 and CH12 channels. From these it is evident that the dominant frequency varies during the seismic action as it is expected for a structure with seismic isolation at the base [Bongiovanni et al, 2017].

6 DYNAMIC TEST ON SEISMIC HDRB ISOLATOR

In order to know the actual characteristics of the isolator for deformations less than 5%, which usually are not tested, due the minor relevance respect to collapse prevention and life safety conditions, a test was performed on the same isolators used for the Type Test of the isolators mounted on the structure under examination, using as input data the relative displacements between the isolated structure and the ground, deriving from the double integration of the accelerations recorded by the "CH03" accelerometer, located at the base of structure and integral to the ground and the barycentric displacement of the structure, calculated by mediating the movements deriving from the recordings of the accelerometers "CH07" and "CH09" placed in correspondence of the first scaffold, in diametrically position opposite, just above the elastomeric isolators.

The registrations for the TP151 event were used for the test.

The event TP151 is the recording, of the accelerometers installed on the structure, of the event of the day 30/10/2016, time 06:40:17, of magnitude Moment (M_w) of 6.5, with an epicenter at a distance of about 36 Km, near Norcia (PG).

The deformation of the test is below 5% deformation of the isolator, the height of the isolator is equal to 240 mm.

The results obtained from the test are shown in the shift-force graph (figure 15): in blue are shown the curves related to the test with the time history obtained from the data of the event TP151 while the curves in red are those related to a test of type Type-Test for a 5% deformation performed at constant frequency.

It can be worthily noticed that displacement is really very low (6 mm instead of the usual 200 – 300 mm in life safety or collapse prevention condition).

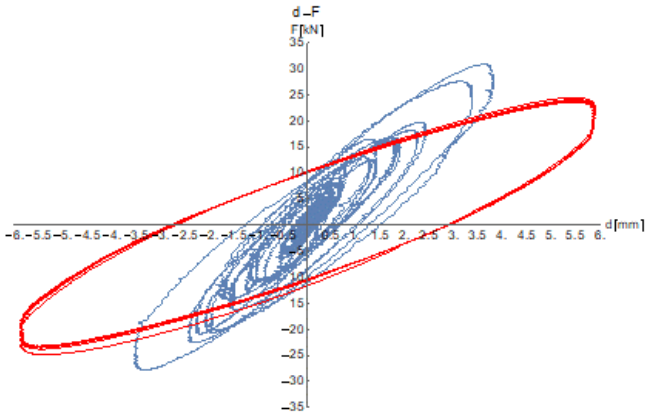

Figure 15. curves related to the test with the time history obtained from the data of the event TP151

7 A COMPUTATIONAL COMPARISON OF NON LINEAR ANALYSIS WITH RECORDED DATA

To verify the reliability of the law and analyse the structure's behaviour, a nonlinear finite element model of the structure was analysed (figure 16).

The definition of a model that is correct and adherent to that which is the real situation is a very complex operation, also through the model to assess, in the most likely way possible, by using the load condition acting on the structure at the time when of the recorded events.

On the model a nonlinear dynamic time history analysis was conducted, (considering the first 50 modes of vibration of the structure), using as input the time histories in terms of acceleration recorded directly on the structure.

An optimization of the model has been performed by inserting the nonlinear behavior of the elastomeric isolator .

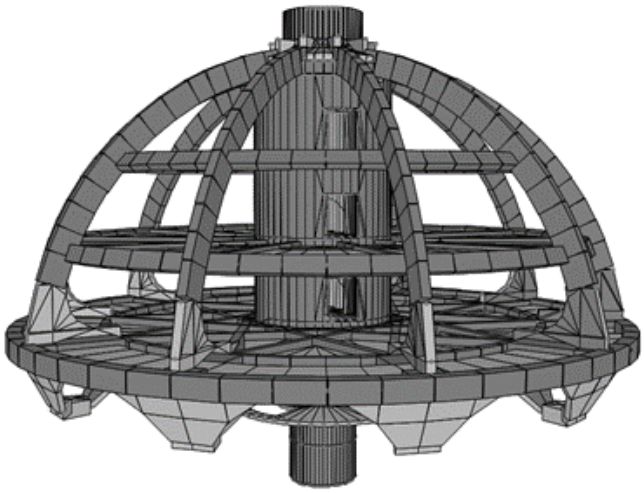

Figure 16. Set view of the computational model

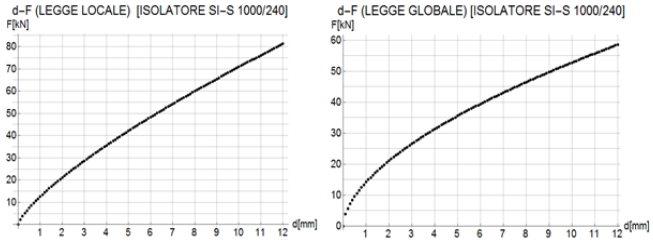

Figure 17. Local and global isolator nonlinear curves

The optimization has been performed by using the laws obtained from the results of the test, performed on the isolator based on the displacement recordings of the TP151 event.

The laws have been appropriately discretized in a number of points with step 1 mm and have been considered in the model (figure 17). The results were then extrapolated in terms of displacement and acceleration of the same points where the accelerometers used in the monitoring are compared with the actual recordings of accelerations and displacement recorded during the analyzed events.

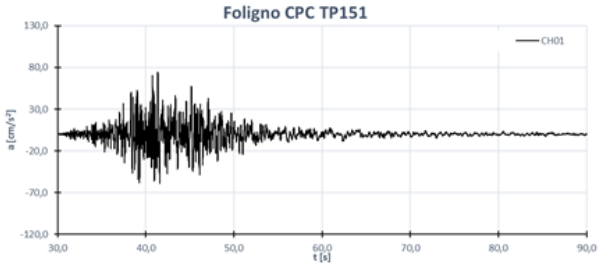

Figure 18. Nonlinear input acceleration TP151 CH01

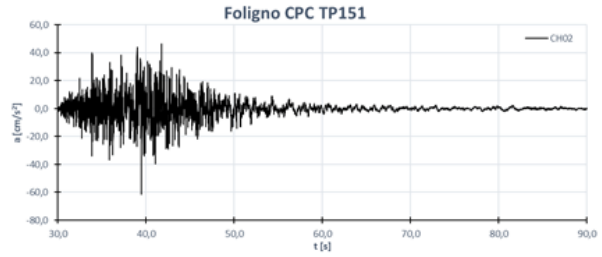

Figure 19. Nonlinear input acceleration TP151 CH02

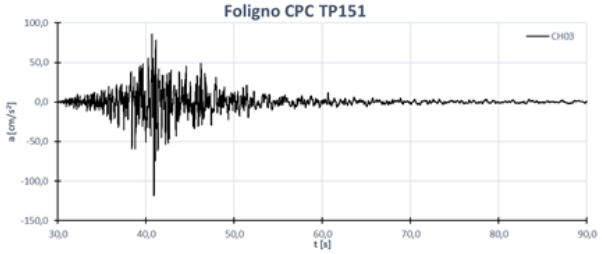

Figure 20. Nonlinear input acceleration TP151 CH03

It is well known that the orientation of the accelerometers with respect to the structure is the same even within the model and in particular the CH03 is oriented in the model according to the X-axis; the CH01 is oriented in the model according to the Y-axis; the CH02 is oriented in the model according to the Z-axis The results of the various analyses carried out are discussed below.

The time history of the recording at the base, in terms of acceleration, of the event named TP151, was considered in the finite element model, as input data by taking into account acceleration time histories acting simultaneously (figure 18, 19, 20).

Some of the results obtained for displacement, compared with the recordings made on the structure, put into evidence the optimal coincidence recorded data with computational analysis (figure 21, 22).

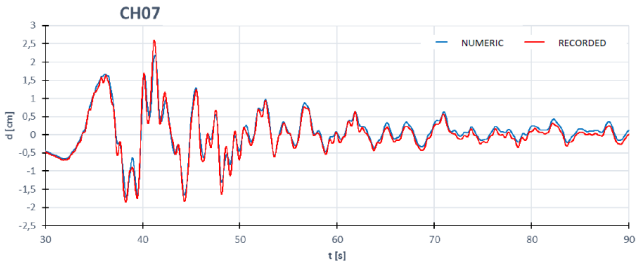

Figure 21. Comparison of recorded displacement with numeric ones

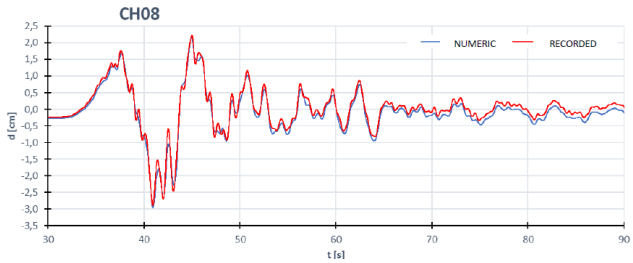

Figure 22. Comparison of recorded displacement with numeric ones

Also the results obtained for acceleration have been compared, as in the previous case, with the recorded time history relevant to the structure:

It can be seen (figure 23) that the model, equipped with the non-linear law of the isolator, has an excellent correspondence with the recorded data.

It's worth noticing, above all, how, in acceleration terms, it reveals a frequency, in most cases, almost equal to the one recorded, but the computational model reveals slightly lower values (the model underestimates the acceleration values, figure 24).

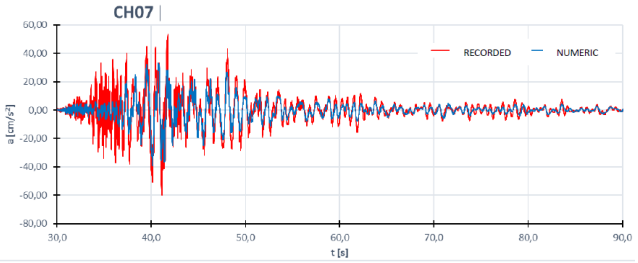

Figure 23. Comparison of recorded acceleration with numeric ones

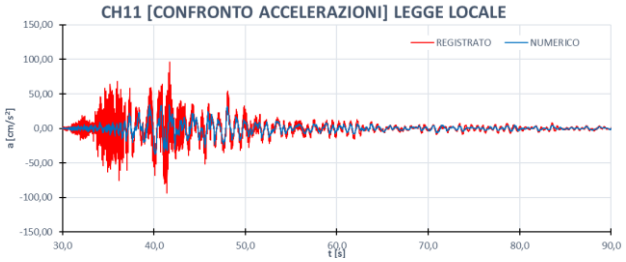

Figure 24. Comparison of recorded acceleration with numeric ones

As in the previous case, even the model implemented with the global law turns out to have a good correspondence with the recordings.

It is worthwhile to point out the effectiveness of the model and the implementation of the latter with the non-linear characteristics of the isolator, by performing a linear analysis.

In the linear analysis the equivalent horizontal stiffness of isolators K_e = 1.31 KN/mm is considered, also considering the acceleration recordings of the TP151 event in the three main directions as input data, expecially in order to validate the usual hypothesis of linear behaviour of rubber isolators.

The results on two channels at the level of the first deck, one in the X-direction (CH09) and another in the Y-direction (CH08) reveal a substantial but not perfect, coincidence, both in term of displacement (figure 25) and I term of acceleration (figure 26).

The differences between linear analysis with K_e and the analysis with the non-linear characteristics of the isolator are very pronounced.

As for displacement (figure 27), the highest recorded peak is more or less reached but the trend does not align with the movements recorded.

As for acceleration (figure 28), however, it is noticed that the numerical solution obtained by performing the linear analysis heavily underestimates the acceleration of the structure, and the time sequence of the accelerations isn't in agreement with the recorded time history.

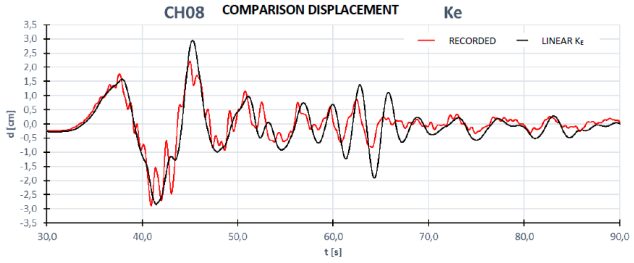

Figure 25. Comparison of displacement between linear analysis and recorded data (CH8)

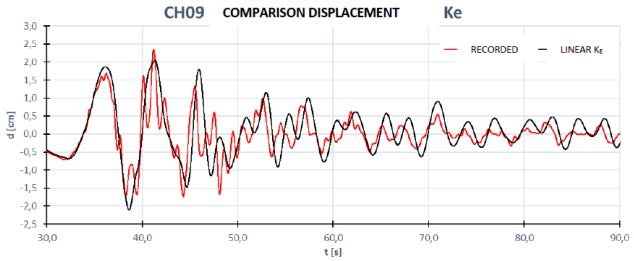

Figure 26. Comparison of displacement between linear analysis and recorded data (CH9)

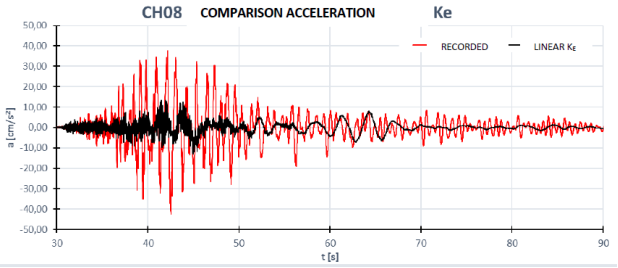

Figure 27. Comparison of acceleration between linear analysis and recorded data (CH8)

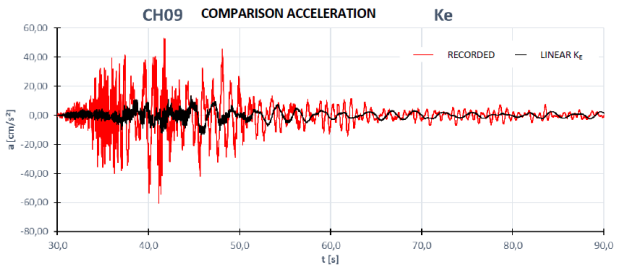

Figure 28. Comparison of acceleration between linear analysis and recorded data (CH9)

There is also a preponderant frequency within the accelerations of the model, certainly different from that recorded on the actual structure.

So the linear response, under low intensity earthquakes, severely underestimates the acceleration on the structure, which can be relevant to the damage of non-structural elements (infills or plant).

Internal resonances of the superstructure seem to play a role in the bad agreement of results in terms of acceleration, in particular in the linear analysis.

8 CONCLUSION

For the structure in question, amplification phenomena have been noticed, up to about twice the acceleration on the superstructure, for very low input energy values. In these cases, however, it is observed that the amplified accelerations are extremely small entities, and very far from damaging the structure.

This is because, as seen, isolation systems with high-damping elastomeric isolators have a stiffness that increases as the deformation decreases (as required to avoid disturbing vibrations even under weak horizontal loads such as wind, etc.), with nonlinear performance; in the case of low-energy seismic input, the isolating system is more rigid even than the equivalent horizontal stiffness K_e.

However, the isolation devices have been shown to function also in low stress conditions, with frequencies higher than those for which they were designed, but still carrying out a filter function.

In fact, less than extremely low acceleration, there is no upward acceleration amplification. It can be observed, from the recorded data, the presence of a frequency cluster different from that of the fixed-base structure.

At the same time, it was also verified that the stresses on the structure were less than those of design.

The recordings of ENEA's permanent accelerometric network, installed on the test structure, and the test carried out on the same isolators used for the qualification, have been analyzed to describe the behavior of isolators in terms of force and displacement by defining two non-linear laws, derived from experimental data.

Obviously, while the first local law seems more suitable to describe the behavior of the isolator for deformations below 5%, the global law is also suitable for condition in which the isolator is deformed even beyond that value.

The developed finite element model is very faithful to what is the actual behavior of the structure and, accompanied by the non-linear laws of the isolator, has a very good feedback with the experimental measurements of seismic events. Consider however that usually there is no coincidence between the results of the numerical model match with the recording ones, because, of course, there are many other variables to consider in a simple model, with particular reference to acceleration results.

By performing linear analyses using the equivalent horizontal stiffness modulus, and comparing the results with the recordings of low

energy seismic events, there are major differences, especially in terms of accelerations that are considerably undervalued (75% less than about).

The differences between the two analyses decrease in the case of higher-entity input accelerations, as could be seen by repeating the linear analysis in the case of the Norcia earthquake, considering the structure in the epicentral zone.

The structure also lends itself very well to this type of analysis, both for a geometric factor being essentially a half sphere, and because it appears to have an extremely rigid superstructure.

The comparison between experimental displacement and computational ones reveals a good agreement, while the comparison relevant to acceleration evidences differences in the range of higher amplitudes, while there is good fitting for lower amplitude values. The reason can be explained in terms of internal structure resonances, which are significant (referring to low level acceleration input) for this structure, as evidenced by the response spectra secondary resonances.

REFERENCES

Salvatori A., Di Cicco A, Clemente P., 2019. Seismic monitoring of buildings with base isolation, *COMPDYN 2019, 7th ECCOMAS Thematic Conference on Computational Methods in Structural Dynamics and Earthquake Engineering*, M. Papadrakakis, M. Fragiadakis (eds.), June 24th – 26th, **2019**, Crete, Greece

Clemente P., 2002. *L'analisi dinamica sperimentale nella salvaguardia dei beni culturali*. ENEA, Roma, ISBN 88-8286-012-4.

Çelebi M., Bazzurro P., Chiaraluce L., Clemente P., Decanini L., De Sortis A., Ellsworth W., Gorini A., Kalkan E., Marcucci S., Milana G., Mollaioli F., Olivieri M., Paolucci R., Rinaldis D., Rovelli A., Sabetta F. and Stephens C., 2010. "Recorded Motions of the Mw6.3 Apr. 6, 2009 L'Aquila (Italy) Earth. and Implications for Building Structural Damage: A Review". *Earth. Spectra*, Vol. **26**, No. 3, 651-684, Aug. 2010, EERI.

Clemente P. and Buffarini G., 2010. "Base isolation: design and optimization criteria". *J. of Seismic Isolation and Protection Systems*, **1-1**(2010), 17-40, Mathematical Science Publisher, DOI 10.2140.siaps.2010.1.17.

Martelli A., Clemente P., Saitta F. and Forni M., 2012. "Recent worldwide application of seismic isolation and energy dissipation to steel and other materials structures and conditions for their correct use". In Mazzolani F.M. & Herrera R. (eds) STESSA 2012 (*Proc., Seventh Int. Conf. Structures in Seismic Areas,* Santiago del Chile, 9-11 Jan), Keynote Lecture, Taylor & Francis Group, London, ISBN 978-0-415-62105-2.

Martelli A., Clemente P., 2015. "Need for an Adequate Seismic Monitoring of Seismically Isolated Buildings to Ensure Safety During Their Life". In De Stefano A. (ed), *Proc. 7th Int. Conf. on Structural Health Monitoring of Intelligent Infrastructure* (SHMII-7, 1-3 July 2015, Turin), RS2, ISHMII & Politecnico di Torino.

Bongiovanni G., Buffarini G., Clemente P., Saitta F., De Sortis A., Nicoletti M., Rossi G., 2015. "Behaviour of the base isolated Jovine School in San Giuliano di Puglia, Italy, under the December 20th 2013 earthquake". *Proc. 14th World Conf. on Seismic Isolation, Energy Dissipation and Active Vibration Control of Structures* (San Diego, Sep 9-11 2015), Univ. of California San Diego, CA USA.

De Stefano A., Matta E., Clemente P., 2016. "Structural health monitoring of historical heritage in Italy: some relevant experiences". *J. of Civil Structural Health Monitoring*, Vol. **6**, No. 1, 83-106, Springer, DOI 10.1007/s13349-016-0154-y (published on line 23 Feb 2016).

Bongiovanni G., Buffarini G., Clemente P., Saitta F., Serafini S., Felici P., 2016. "Ambient vibration analysis of a strategic base isolated building". *Proc. 6th Int. Civil Struct. Health Monitoring Workshop* (CSHM-6, Belfast, 26-27 May, 2016), Queen's University Belfast.

Clemente P., Bongiovanni G., Buffarini G. and Saitta F., 2016. "Experimental analysis of base isolated buildings under low magnitude vibrations". *Int. J. of Earthquake and Impact Engineering*, Vol. **1**, No. 1-2, 199-223, Inderscience Publishers, DOI: 10.1504/IJEIE.2016.10000961.

Martelli A., Clemente P., Benzoni G., 2017. "State-of-the-art of development and application of anti-seismic systems in Italy". *Proc. New Zealand Society for Earthquake Annual Conf. and 15th World Conf. on Seismic Isolation, Energy Dissipation and Active Vibration Control of Structures* (NZSEE2017 and 15WCSI, Wellington, Apr 27-29).

Clemente P., Bongiovanni G., Benzoni G., 2017. "Monitoring of seismic isolated buildings: state of the art and results under high and low energy inputs". *Proc. New Zealand Society for Earthquake Annual Conf. and 15th World Conf. on Seismic Isolation, Energy Dissipation and Active Vibration Control of Structures* (NZSEE2017 and 15WCSI, Wellington, Apr 27-29).